Organic Electronics

DOI: 10.1002/anie.201101021

Enhancement of Donor–Acceptor Polymer Bulk Heterojunction Solar Cell Power Conversion Efficiencies by Addition of Au Nanoparticles**

Dong Hwan Wang, Do Youb Kim, Kyeong Woo Choi, Jung Hwa Seo, Sang Hyuk Im, Jong Hyeok Park, O Ok Park,* and Alan J. Heeger**

Polymer-fullerene-based bulk heterojunction (BHJ) solar cells with large surface areas can be fabricated by using low-cost roll-to-roll manufacturing methods.[1–11] However, because of the low mobility of BHJ materials, there is competition between the sweep-out of the photogenerated carriers by the built-in potential and recombination of the photogenerated carriers within the thin BHJ film;[12–15] useful film thicknesses are limited by recombination.[16] Thus, there is a need to increase the absorption by the BHJ film without increasing the film thickness. Metal nanoparticles exhibit localized surface plasmon resonances (LSPR) that couple strongly to the incident light. In addition, relatively large metallic nanoparticles can reflect and scatter light and thereby increase the optical path length within the BHJ film. Thus, the addition of metal nanoparticles to BHJ films offers the possibility of enhanced absorption and correspondingly enhanced photogeneration of mobile carriers; moderate increases in power-conversion efficiency (PCE) have been reported.[17–20] To ensure that the Au nanoparticles have a positive effect, it is important to reduce exciton quenching by nonradiative energy transfer between the active layer and Au nanoparticles. Hence, most researchers add the metal nanoparticles at the interface of the indium tin oxide (ITO) anode and the active layer or embed them in the poly(3,4-ethylenedioxythiophene):poly(styrene sulfonate) (PEDOT:PSS) layer.[21] However, direct mixing of metal nanoparticles in an active layer would be attractive because, in principle, it could reduce the cell resistance and incident light could not be reflected by the metal nanoparticles that are embedded in ITO or the PEDOT:PSS layer before reaching the active layer.

Herein we report the results of a study that demonstrates several positive effects that arise from the addition of Au nanoparticles with an approximate size of 70 nm to BHJ photovoltaic cells fabricated from poly(3-hexylthiophene) (P3HT)/[6,6]-phenyl C_{70} butyric acid methyl-ester ($PC_{70}BM$), poly[N-9″-hepta-decanyl-2,7-carbazole-alt-5,5-(4′,7′-di-2-thienyl-2′,1′,3′-benzothiadiazole) (PCDTBT)/$PC_{70}BM$, and poly{[4, 4′-bis(2-ethylhexyl) dithieno(3,2-b:2′,3′-d)silole]-2,6-diyl-alt-[4,7-bis(2-thienyl)-2,1,3-benzothiadiazole]-5,5′-diyl} (Si-PCPDTBT)/$PC_{70}BM$ (Figure 1). Using solution chemistry, we synthesized truncated octahedral Au nanoparticles (see the scanning electron microscopy (SEM) image in Figure 1c and Figure S1 in the Supporting Information) with an average diameter of approximately 70 nm.[22] The Au nanoparticles were blended into a BHJ solution with different weight ratios. At the optimized blend ratio (5 wt% Au nanoparticles), the PCE increased from 3.54% to 4.36% (P3HT/$PC_{70}BM$), from 5.77% to 6.45% (PCDTBT/$PC_{70}BM$), and from 3.92% to 4.54% (Si-PCPDTBT/$PC_{70}BM$).

Earlier research on metal nanoparticles incorporated into organic photovoltaic devices focused on relatively small particles with diameters less than 10 nm. However, the use of larger Au nanoparticles is expected to lead to several positive effects. Individual Au nanoparticles can act as hole conductors because their work function is well matched with the energy of the highest occupied molecular orbital (HOMO) of P3HT. Therefore, large Au nanoparticles can transport holes more efficiently because there are fewer interfaces between Au and the active layer. Because large Au particles can reflect and scatter the incident light more efficiently than small Au nanoparticles, more effective light harvesting is expected.

Figure 1 and Figure S1 show the molecular structures, photovoltaic device structure, energy level diagrams of PCDTBT, Si-PCPDTBT, P3HT, and $PC_{70}BM$, and the SEM

[*] D. H. Wang, Dr. J. H. Seo, Prof. A. J. Heeger
Center for Polymers and Organic Solids
University of California at Santa Barbara
Santa Barbara, CA 93106 (USA)
Fax: (+1) 805-893-4755
E-mail: ajhe@physics.ucsb.edu

D. H. Wang, D. Y. Kim, K. W. Choi, Prof. O. O. Park
Department of Chemical and Biomolecular Engineering
Korea Advanced Institute of Science and Technology
(BK 21 Graduate Program)
373-1 Guseong-dong, Yuseong-gu, Daejeon 305-701
(Republic of Korea)
Fax: (+82) 42-350-3910
E-mail: ookpark@kaist.ac.kr

Dr. S. H. Im
KRICT-RPFL Global Research Laboratory, Advanced Materials Division, Korea Research Institute of Chemical Technology
Daejeon (Republic of Korea)

Prof. J. H. Park
School of Chemical Engineering and
SKKU Advanced Institute of Nanotechnology (SAINT)
Sungkyunkwan University, Suwon 440-746 (Republic of Korea)
Fax: (+82) 31-290-7272
E-mail: lutts@skku.edu

[**] This research was supported by Future-based Technology Development Program (Nano Fields, 2010-0029321) and the WCU (World Class University) program (R32-2008-000-10142-0) through the NRF of Korea funded by the MEST. J. H. Park acknowledges the support from NRF of Korea funded by the MEST (NRF-2009-C1AAA001-2009-0094157, 2011-0006268). Research at UCSB was supported by the US Army General Technical Services (LLC/GTS-S-09-1-196) and by the Department of Energy (BES-DOE- ER46535).

Supporting information for this article is available on the WWW under http://dx.doi.org/10.1002/anie.201101021.

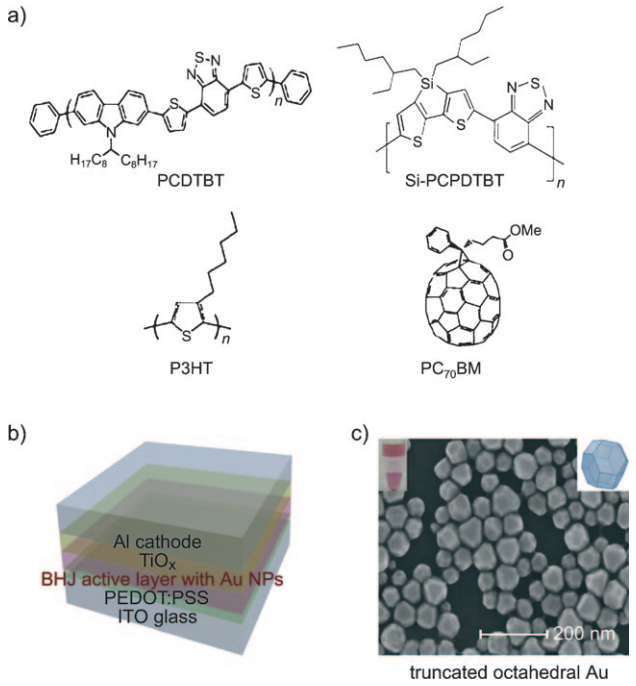

Figure 1. a) Molecular structures of photovoltaic materials (donors: PCDTBT, Si-PCPDTBT, P3HT; acceptor: $PC_{70}BM$); b) schematic of a photovoltaic device; and c) SEM image of truncated octahedral Au nanoparticles.

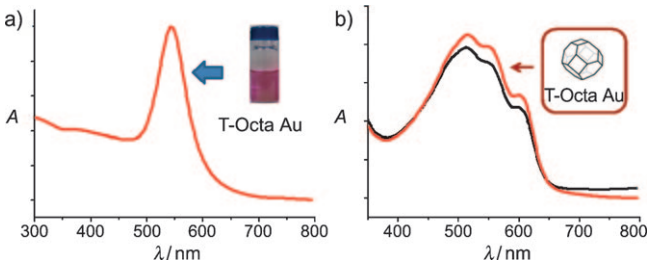

Figure 2. UV/Vis spectra of a) truncated octahedral Au nanoparticles with maximum absorption peaks of near 530 nm b) plain BHJ film (black curve) and BHJ film with truncated octahedral shape, weight ratio of 5 wt% (red curve) for the P3HT/$PC_{70}BM$ after thermal annealing at 150 °C for 20 min.

image of the synthesized truncated octahedral Au nanoparticles. PCDTBT has a relatively deep HOMO energy (ca. 5.5 eV), which leads to a higher open-circuit voltage (V_{OC}).[23] Si-PCPDTBT has higher crystallinity.[24]

In typical colloidal chemistry that involves the synthesis of Au nanoparticles, *N*,*N*-dimethylformamide (DMF) is used as a solvent and as reducing agent for Au salts (see the Supporting Information). Au atoms can then be successfully obtained by reducing tetrachloroaurate trihydrate ($HAuCl_4{\cdot}3H_2O$) with DMF in the presence of deionized water:[25] when the concentration of Au atoms reaches super saturation, Au particles are nucleated and nanoparticles are formed after the dissociation and reduction of the Au salt. During the growth of the nanoparticles, poly(vinylpyrrolidone) (PVP) prevents the growth of Au on other facets, thereby acting as a capping agent to control the shape of the particles.[22] The water content is a critical factor that determines, whether Au nanoparticles are octahedral or truncated octahedral. Water enables the Au salts to dissociate into Au ions that can be readily converted to Au atoms by DMF.[26]

Figure 2a and b show UV/Vis absorption spectra of the truncated octahedral Au nanoparticles and the P3HT/$PC_{70}BM$ BHJ active layer with Au nanoparticles. Uniformly sized truncated octahedral Au nanoparticles were successfully synthesized by controlling the water content and the concentration of PVP, DMF, and the Au precursor. Energy dispersive spectroscopy (EDS) analysis showed that the Au nanoparticles consist of pure gold. Before spincasting of the polymer solution blended with Au, it was necessary to disperse the nanoparticles in the solution so that they could be better dispersed in the BHJ film. A polymer solution blended with Au nanoparticles was therefore subjected to ultrasonic agitation for 10 min and then directly spincast in a glove box. Figure 2b confirms that after being annealed at 150 °C for 20 min, the P3HT/$PC_{70}BM$ (with 5 wt% of truncated octahedral Au nanoparticles) shows greater optical absorbance than the P3HT/$PC_{70}BM$ blended BHJ film. We suggest that the Au nanoparticles can act as an effective "optical reflector" for solar light. Multiple reflections will cause the light to pass through the BHJ film several times.[27]

Figure 3a–c shows the photocurrent–voltage (*J*–*V*) curves of devices with the optimized weight ratio of 5 wt% of truncated octahedral Au nanoparticles depending on the photovoltaic material used (P3HT/$PC_{70}BM$, PCDTBT/$PC_{70}BM$, and Si-PCPDTBT/$PC_{70}BM$). The P3HT/$PC_{70}BM$ BHJ device with truncated octahedral Au nanoparticles exhibits a power conversion efficiency of 4.36% (V_{OC} = 0.63 V, short-circuit current: $J_{SC} = 11.18\ mA\,cm^{-2}$, fill factor: $FF = 0.61$, Figure 3a). The optimum ratio of 5 wt% Au nanoparticles in BHJs of P3HT/$PC_{70}BM$ provided the best efficiency (Figure S2a). Figure S2b,d shows SEM and AFM images of BHJ films blended with truncated octahedral Au nanoparticles. The SEM images reveal that the nanoparticles are almost uniformly dispersed in the BHJ film and are clearly coated on the substrate.

Figure 3b and c show the *J*–*V* curves for PCDTBT and Si-PCPDTBT, with and without 5 wt% truncated octahedral Au nanoparticles. Figure 3b and c compare the *J*–*V* curves of the reference PCDTBT/$PC_{70}BM$ based on devices with a layer thickness of 120 nm or Si-PCPDTBT/$PC_{70}BM$ BHJ based on devices with a thickness of 150 nm with the ones that contain the truncated octahedral Au nanoparticles. The PCDTBT/$PC_{70}BM$ device with 5 wt% of Au nanoparticles has a PCE of 6.45% ($V_{OC} = 0.89$ V, $J_{SC} = 11.16\ mA\,cm^{-2}$, and $FF = 0.65$); the Si-PCPDTBT/$PC_{70}BM$ device has a PCE of 4.54% (V_{OC} = 0.57 V, $J_{SC} = 13.13\ mA\,cm^{-2}$, and $FF = 0.61$).

The device efficiencies with these two types of donor materials are closely related to the thickness of the BHJ active layer, therefore it is very important to confirm the relation between the BHJ thickness and the performance of the solar cell. The average reference device efficiency with PCDTBT/$PC_{70}BM$ with an optimized thickness of approximately 90 nm is 6.11%, while thinner (less than 60 nm) or thicker (more than 120 nm) layers show decreased efficiency with reduced

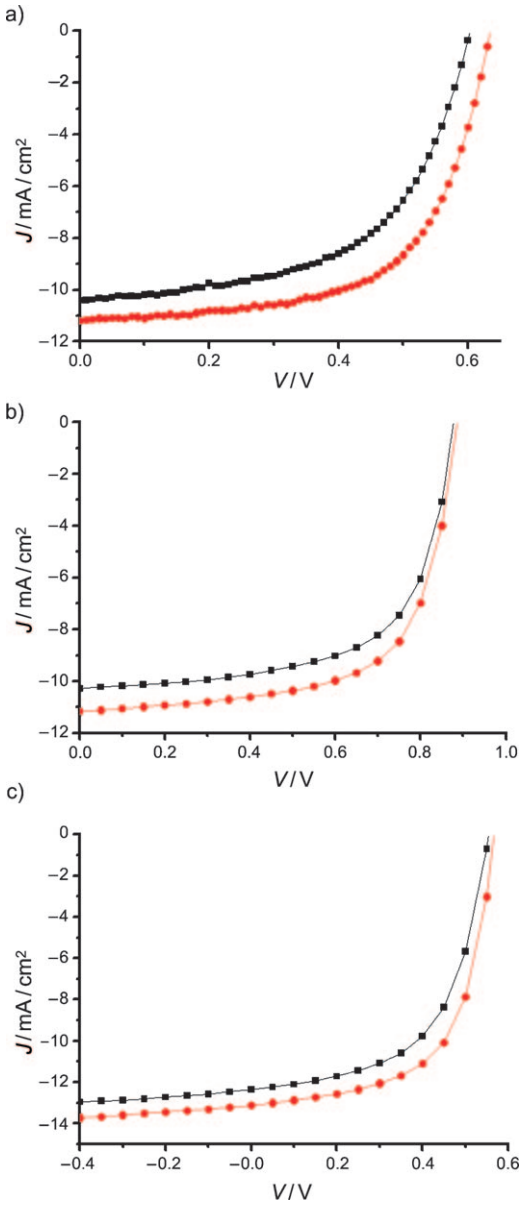

Figure 3. *J–V* curves of devices with plain BHJ (black curves) or BHJ with 5 wt% Au nanoparticles (red curves) depending on photovoltaic materials a) P3HT/PC_{70}BM BHJ (ca. 220 nm), b) PCDTBT/PC_{70}BM BHJ (ca. 120 nm), and c) Si-PCPDTBT/PC_{70}BM BHJ (ca. 150 nm).

J_{SC}. The average reference device efficiency with Si-PCPDTBT/PC_{70}BM with an optimized thickness of approximately 120 nm is 4.28%, while other thicknesses show smaller efficiencies (Figure S3). These results demonstrate that the optimized thickness, which differs for different materials, is a critical factor. However, the optimized devices obtained by controlling the film thickness could not give efficiencies that were obtained from BHJ cells with added Au nanoparticles. The P3HT/PC_{70}BM, PCDBT/PC_{70}BM, and Si-PCPDTBT/PC_{70}BM BHJ devices with Au nanoparticles show improved device performances compared to the optimized reference devices without Au (Figure S3). Therefore, the Au nanoparticles play an important role in the BHJ active layer with several positive effects.

Figure S4 shows the incident photon-to-current efficiency (IPCE) spectra of the reference BHJ cell and the BHJ cell made with 5 wt% of truncated octahedral Au nanoparticles. The improvements in the IPCE result from the Au nanoparticles, particularly from efficient light scattering and improved charge transport. The increased J_{SC} shown in Figure 3 implies that more light is harvested in the active layer because of multiple light scattering by the Au nanoparticles. To confirm this hypothesis we measured optical absorption spectra; the optical absorption could not be determined directly because the Al cathode is not transparent. Therefore, we measured the diffuse reflectance spectra so that we could determine the fraction of incident photons absorbed by the BHJ film. Figure 4 shows diffuse reflectance spectra of the devices fabricated with and without Au nanoparticles in P3HT/PC_{70}BM. The lower reflectivity of the device with Au nanoparticles indicates stronger absorption of the incident light.

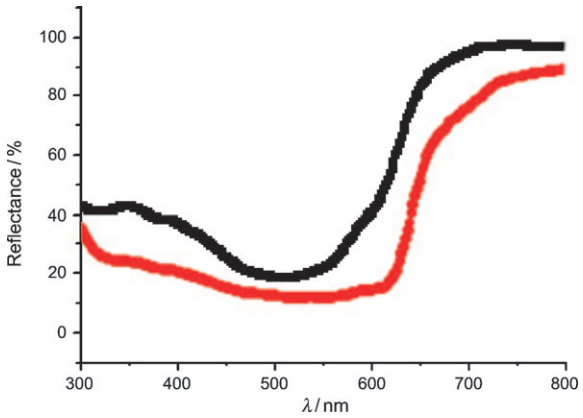

Figure 4. Diffuse reflectance spectra of the devices fabricated with P3HT/PC_{70}BM BHJ (black curve) and P3HT/PC_{70}BM with the addition of 5 wt% truncated octahedral Au nanoparticles.

Figure 5a and b show energy level diagrams of the photovoltaic devices with Au nanoparticles smaller than 10 nm and with Au nanoparticles larger than an average diameter of 70 nm.[28] The Au particles used in this study are expected to have a work function of approximately 5.1 eV (close to the HOMO energy level of P3HT, 5.2 eV), thus resulting in a small energy barrier for hole extraction. As illustrated in Figure 5a and b, the use of these large Au nanoparticles might lead to a reduced series resistance because the holes need to pass through fewer interfaces than in the system with small Au nanoparticles. Ultraviolet photoelectron spectroscopy (UPS) was used to probe the energy levels of blend layers that comprise Au nanoparticles. Figure 5c shows the UPS results for P3HT/PC_{70}BM (blue) and P3HT/PC_{70}BM (red) with Au nanoparticles, using ITO (black) as a reference substrate. Examination of the secondary electron cutoff region in Figure 5c and d (14–18 eV) makes it possible to extract the shift in the vacuum energy level (E_{vac}); the E_{vac} shift is a measure for the magnitude of the interfacial dipole (Δ).[29–33] The deposition of blend layers leads to a shift toward higher binding energies. The blend

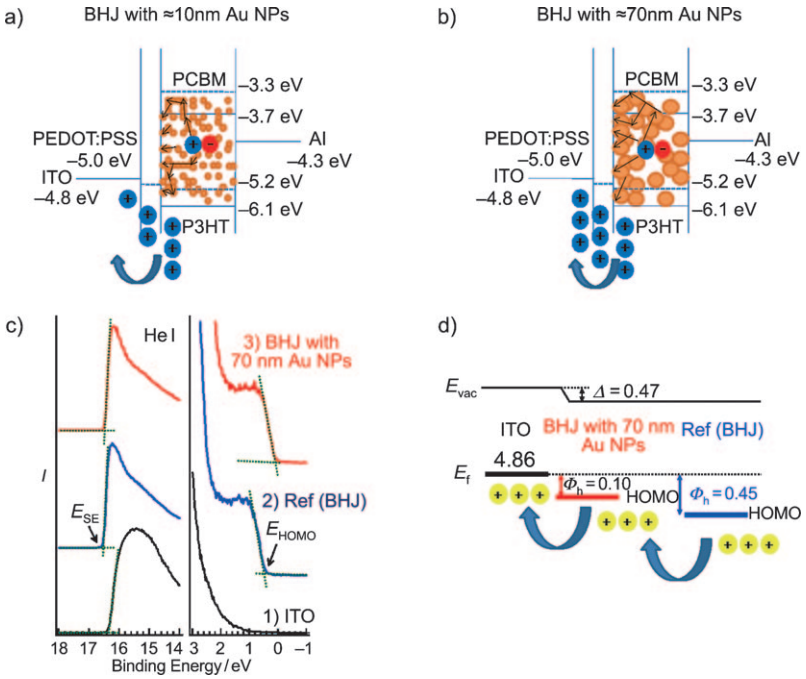

Figure 5. Energy band diagram of photovoltaic devices with Au nanoparticles smaller than 10 nm or larger than the average diameter of 70 nm. UPS spectra and energy diagrams of P3HT/PCBM BHJs or BHJs with Au nanoparticles a) less than 10 nm; b) average diameter larger than 70 nm; c) UPS spectra; d) Energy diagrams of P3HT/PCBM (blue), P3HT/PCBM with Au nanoparticles (red), and an ITO substrate (black). (E_{vac}: vacuum level, E_F: Fermi level, Δ: interfacial dipole, Φ_h: hole-injection barrier).

HOMO energy levels (E_{HOMO}) were determined using the low binding energy region (0–3 eV). The hole injection barrier (Φ_h) is the energy difference between the E_{HOMO} and zero binding energy (relative to the work function of ITO, see Figure 5d); from Figure 5d, $\Phi_h = 0.45$ eV for P3HT/$PC_{70}BM$. Thus, the introduction of Au nanoparticles decreases Φ_h to 0.1 eV. This smaller Φ_h can induce a cascade hole transfer from the HOMO energy of P3HT to the ITO electrode; efficient hole extraction can reduce the possibility of electron/hole recombination, thus resulting in the increase of V_{OC}.

To confirm the enhanced *FF*, the dark *I–V* characteristics were investigated (Figure S5). The dark current of the devices with Au nanoparticles shows a significantly increased shunt resistance, hence resulting in a short-circuit current that is greater than that of the reference device.[34,35] Figure S5a,b indicate that the reduced leakage current is a critical factor in determining the device performance. Also, the series resistances of the devices with added Au nanoparticles decrease from 1.86 Ωcm^2 (without Au) to 1.49 Ωcm^2 (with Au) for PCDTBT/$PC_{70}BM$ and from 2.54 Ωcm^2 (without Au) to 2.18 Ωcm^2 (with Au) for Si-PCPDTBT/$PC_{70}BM$. The reduced series resistance increased the *FF* from 0.64 to 0.65 (PCDTBT/$PC_{70}BM$) and from 0.63 to 0.64 (Si-PCPDTBT/$PC_{70}BM$).

We have demonstrated several positive effects of large Au nanoparticles in organic photovoltaic devices based on P3HT/$PC_{70}BM$, PCDTBT/$PC_{70}BM$, Si-PCPDTBT/$PC_{70}BM$ BHJs. Au nanoparticles with a truncated octahedral structure were synthesized by means of solution chemistry. The use of an optimized concentration, 5 wt%, of truncated octahedral Au nanoparticles in the BHJ film increases the J_{SC}, the *FF*, and the IPCE. These improvements result from a combination of enhanced light absorption caused by the light scattering of Au nanoparticles in the active layer; plasmon-induced light concentration at specific wavelengths, however, was not observed. Moreover, improved charge transport results in low series resistance. For P3HT/$PC_{70}BM$, the PCE increased from 3.54% to 4.36%; for PCDTBT/$PC_{70}BM$, the PCE increased from 5.77% to 6.45%, and for Si-PCPDTBT/$PC_{70}BM$, the PCE increased from 3.92% to 4.54%. These increases in PCE depend in detail on the size of the Au nanoparticles and the optimized weight ratio of the Au nanoparticles in the BHJ film.

The plasmon resonance of octahedral Au nanoparticles is at 603 nm (Figure S6), that of truncated octahedral nanoparticles is at 530 nm. We have carried out similar solar cell experiments using octahedral Au nanoparticles (ca. 70 nm) and have found similar enhancement of the PCE and similar broad band response as for the truncated octahedral nanoparticles (Table S1). We conclude that the local field enhancement from the narrow band plasmon resonances is not the dominant mechanism. The multiple scattering leads to longer optical paths within the BHJ material and is therefore responsible for the enhancement of the PCE.

Experimental Section

Photovoltaic devices based on P3HT/$PC_{70}BM$ with a blend of octahedral or truncated octahedral Au nanoparticles were prepared as shown in Figure 1. Impurities and dust were removed from the ITO glass with an organic solvent, such as chloroform, acetone, and isopropanol. The glass was then treated with oxygen plasma for 10 min to reform the ITO surface. PEDOT:PSS (Baytron P) was spincast onto the ITO in a thickness of 35 nm. The ITO glass with the PEDOT:PSS layer was preheated on a digitally controlled hotplate at 140°C for 10 min. The reference device with a BHJ structure that comprised P3HT and $PC_{70}BM$ with a blend ratio of 1:0.6 was spincast at 900 rpm for 5 seconds in a glove box. The BHJ with the thickness of the reference device or BHJs with weight ratios of 1 wt%, 5 wt%, 10 wt%, and 20 wt% of truncated octahedral Au active layers were observed to be approximately 220 nm from the surface profiler. Also, the devices of PCDTBT/$PC_{70}BM$ and Si-PCPDTBT/$PC_{70}BM$ BHJs or BHJs blended with truncated octahedral Au with optimized 5 wt% weight ratios were spincoated in a thickness of 120 nm (PCDTBT/$PC_{70}BM$) or 150 nm (Si-PCPDTBT/$PC_{70}BM$) on top of the PEDOT/PSS layer. A mixture of PCDTBT/$PC_{70}BM$ (7 mg/28 mg) was dissolved in dichlorobenzene/ chlorobenzene 3:1 (1 mL) and Si-PCPDTBT/$PC_{70}BM$ (7 mg/14 mg) was dissolved in dichlorobenzene (1 mL). The films were dried at 80°C for 10 min in a glove box. Before spincasting, the BHJ active solutions with Au nanoparticles were ultrasonically agitated for 10 min, so that the nanoparticles were well dispersed in the solution. The polymeric TiO_x interlayer was then spincoated to reach a layer thickness of approximately 5 nm and a thermal evaporator was used to uniformly deposit a 100 nm thick Al

metal cathode under a pressure of 1.9×10^{-6} Torr.[7] The P3HT/$PC_{70}BM$ BHJ was subsequently thermally annealed using a hotplate at 150 °C for 20 min in a glovebox. A video microscope system (SOMETECH, SV-35) was used to measure the active areas, and an aperture with an area of 9.84 mm^2 was used on top of the cell to confirm the accuracy of the device area.

Received: February 10, 2011
Published online: April 21, 2011

Keywords: light scattering · nanoparticles · organic electronics · photovoltaics · solar cells

[1] G. Yu, J. Gao, J. C. Hummelen, F. Wudl, A. J. Heeger, *Science* **1995**, *270*, 1789 – 1791.
[2] A. J. Heeger, *Angew. Chem.* **2001**, *113*, 2660 – 2682; *Angew. Chem. Int. Ed.* **2001**, *40*, 2591 – 2611.
[3] J. Peet, M. L. Senatore, A. J. Heeger, *Adv. Mater.* **2009**, *21*, 1521 – 1527.
[4] W. Ma, C. Yang, X. Gong, K. H. Lee, A. J. Heeger, *Adv. Funct. Mater.* **2005**, *15*, 1617 – 1622.
[5] B. C. Thompson, J. M. J. Fréchet, *Angew. Chem.* **2008**, *120*, 62 – 82; *Angew. Chem. Int. Ed.* **2008**, *47*, 58 – 77.
[6] K. Kim, J. Liu, M. A. G. Namboothiry, D. L. Carroll, *Appl. Phys. Lett.* **2007**, *90*, 163511.
[7] D. H. Wang, S. H. Im, H. K. Lee, J. H. Park, O. O. Park, *J. Phys. Chem. C* **2009**, *113*, 17286 – 17273.
[8] G. Dennler, M. C. Scharber, C. J. Brabec, *Adv. Mater.* **2009**, *21*, 1323 – 1338.
[9] C. J. Brabec, N. S. Sariciftci, J. C. Hummelen, *Adv. Funct. Mater.* **2001**, *11*, 15 – 26.
[10] D. H. Wang, H. K. Lee, D. G. Choi, J. H. Park, O. O. Park, *Appl. Phys. Lett.* **2009**, *95*, 043505.
[11] D. H. Wang, D. G. Choi, O. O. Park, J. H. Park, *J. Mater. Chem.* **2010**, *20*, 4910 – 4915.
[12] P. W. M. Blom, V. D. Mihailetchi, L. J. A. Koster, D. E. Markov, *Adv. Mater.* **2007**, *19*, 1551 – 1566.
[13] V. Choong, Y. Park, Y. Gao, T. Wehrmeister, K. Müllen, B. R. Hsieh, C. W. Tang, *Appl. Phys. Lett.* **1996**, *69*, 1492.
[14] D. E. Markov, E. Amsterdam, P. W. M. Blom, A. B. Sieval, J. C. Hummelen, *J. Phys. Chem. A* **2005**, *109*, 5266 – 5274.
[15] S. K. Hau, H. L. Yip, O. Acton, N. S. Baek, H. Ma, A. K. Y. Jen, *J. Mater. Chem.* **2008**, *18*, 5113 – 5119.
[16] S. H. Park, A. Roy, S. Beaupré, S. Cho, N. Coates, J. S. Moon, D. Moses, M. Leclerc, K. Lee, A. J. Heeger, *Nat. Photonics* **2009**, *3*, 297 – 303.
[17] D. Derkacs, S. H. Lim, P. Matheu, W. Mar, E. T. Yu, *Appl. Phys. Lett.* **2006**, *89*, 093103.
[18] R. B. Konda, R. Mundle, H. Mustafa, O. Bamiduro, A. K. Pradhan, U. N. Roy, Y. Cui, A. Burger, *Appl. Phys. Lett.* **2007**, *91*, 191111.
[19] K. Kim, D. L. Carroll, *Appl. Phys. Lett.* **2005**, *87*, 203113.
[20] A. Gole, C. J. Murphy, *Chem. Mater.* **2005**, *17*, 1325.
[21] J. H. Lee, J. H. Park, J. S. Kim, D. Y. Lee, K. Cho, *Org. Electron.* **2009**, *10*, 416 – 420.
[22] D. Y. Kim, S. H. Im, O. O. Park, Y. T. Lim, *CrystEngComm* **2010**, 12, 116 – 121.
[23] M. C. Scharber, D. Mühlbacher, M. Koppe, P. Denk, C. Waldauf, A. J. Heeger, C. J. Brabec, *Adv. Mater.* **2006**, *18*, 789 – 794.
[24] M. C. Scharber, M. Koppe, J. Gao, F. Cordella, M. A. Loi, P. Denk, M. Morana, H.-J. Egelhaaf, K. Forberich, G. Dennler, R. Gaudiana, D. Waller, Z. Zhu, X. Shi, C. J. Brabec, *Adv. Mater.* **2010**, *22*, 367 – 370.
[25] A. V. Gaikwad, P. Verschuren, S. Kinge, G. Rothenberg, E. Eiser, *Phys. Chem. Chem. Phys.* **2008**, *10*, 951 – 956.
[26] J. Xu, S. Li, J. Weng, X. Wang, Z. Zhou, K. Yang, M. Liu, X. Chen, Q. Cui, M. Cao, Q. Zhang, *Adv. Funct. Mater.* **2008**, *18*, 277 – 284.
[27] H. A. Atwater, A. Polman, *Nat. Mater.* **2010**, *9*, 205- 213.
[28] C. P. Vinod, G. U. Kulkarni, C. N. R. Rao, *Chem. Phys. Lett.* **1998**, *289*, 329 – 333.
[29] S. Braun, W. R. Salaneck, M. Fahlman, *Adv. Mater.* **2009**, *21*, 1450 – 1472.
[30] I. G. Hill, D. Milliron, J. Schwartz, A. Kahn, *Appl. Surf. Sci.* **2000**, *166*, 354 – 362.
[31] J. H. Seo, R. Yang, J. Z. Brzezinski, B. Walker, G. C. Bazan, T.-Q. Nguyen, *Adv. Mater.* **2009**, *21*, 1006 – 1011.
[32] Y. Gao, *Acc. Chem. Res.* **1999**, *32*, 247 – 255.
[33] H. Ishii, K. Sugiyama, E. Ito, K. Seki, *Adv. Mater.* **1999**, *11*, 605 – 625.
[34] J. H. Lee, S. Cho, A. Roy, H.-T. Jung, A. J. Heeger, *Appl. Phys. Lett.* **2010**, 96, 163303.
[35] P. Schilinsky, C. Waldauf, C. J. Brabec, *Adv. Funct. Mater.* **2006**, *16*, 1669 – 1672.

